

Trigger efficiency for supersymmetric channels in ATLAS

Valentina Ferrara

September 2007

Contents

1	Introduction	2
1.1	Supersymmetry Overview	2
1.2	Supersymmetric Models	3
1.3	SUSY at LHC	4
2	SUSY studies	5
2.1	Data sample	5
2.2	l^+l^- signatures	5
2.3	Reconstruction of gluinos and squarks	6
3	Trigger efficiency	7
3.1	l^+l^- signatures	8
3.2	Trigger efficiency and turn-on curves	9
3.3	Missing Transverse Energy Reconstruction	11
4	Summary	12

1 Introduction

The Standard Model (SM) is the name given to the best current mathematical description of the subatomic particles and the forces between them. It has been extremely successful at explaining and predicting the results of a wide range of experiments.

However, the SM has been regarded only as a low-energy effective theory of a yet-more-fundamental one. There are several good reasons to suppose this: for instance it cannot explain the existence of the dark matter, which makes up approximately one quarter of the energy density of the universe.

Perhaps the most obvious argument is that it does not include the gravitational force. This precludes it from describing interactions at arbitrarily high energies.

A related puzzle is the huge difference in the strengths of the electroweak and gravitational forces: it seems unnatural for gravity to be so much weaker than the other gauge forces.

This is what is known as the hierarchy problem and arises from the one-loop quantum corrections to the Higgs 'bare mass'. These are quadratically divergent and set the Higgs bare mass at GUT/Planck scale. Since the SM predicts the physical Higgs mass to be around 100 GeV , an enormous 'fine-tuning' to the parameters of the bare Lagrangian is required.

Another interesting question is whether there's a reason why the fermions have a mass spectrum which stretches over almost six orders of magnitude between the electron and the top quark, or an explanation for having three families of quarks and leptons.

These and other arguments represent the belief that there is physics beyond the SM.

1.1 Supersymmetry Overview

Supersymmetry is one of the most proposed new choices for new physics beyond the Standard Model and resolves several of the issues previously raised (though not all of them). The basic idea is that an additional symmetry is introduced to the theory such that the Lagrangian is invariant under transformations which convert fermions into bosons and vice versa. This immediately doubles the number of particles and more importantly helps to solve the hierarchy problem: in fact, an equal number of bosons and fermions, which give opposite signs in loops, cancel the quadratic divergences.

If supersymmetry were an exact symmetry, then particles and their superpartners would be degenerate in mass.

Since superpartners have not (yet) been observed, supersymmetry must also be broken. Nevertheless, the stability of the gauge hierarchy can still be maintained if the supersymmetry breaking is *soft*, which means that the breaking terms are non-

supersymmetric ones in the Lagrangian that are either linear, quadratic or cubic in the fields, and the corresponding supersymmetry-breaking mass parameters are no larger than a few TeV . The most interesting theories of this type are theories of "weak-scale" supersymmetry, where the effective scale of supersymmetry breaking is tied to the scale of electroweak symmetry breaking.

In the perturbative SM, the baryon and lepton numbers are conserved whereas, in supersymmetric theories, it is possible to violate both. This violation is strongly constrained by experiment: for example, a weak-scale proton decay would take place. Since the proton is remarkably stable, the solution is the imposition of the multiplicative $R - Parity$:

$$R = (-1)^{3(B-L)+2S} \quad (1)$$

where: B is the baryonic number, L is the leptonic number and S is the spin of the particle. This combination of quantum numbers ensures that the SM particles have $R = +1$ whereas their superpartners have $R = -1$. This has the consequence that susy particles can only be produced in pairs and must decay to states which also contain an odd number of susy particles, with the result that the lightest supersymmetric particle (LSP), which must eventually be produced at the end of a decay chain, is stable. Each SUSY event must then produce an even number of LSPs. In order to be consistent with cosmological constraints, the latter are almost certainly electrically and color neutral. Consequently, the LSP is weakly interacting with ordinary matter. Thus, the canonical signature for R-Parity-conserving supersymmetric theories is missing (transverse) energy, due to the escape of the LSP.

1.2 Supersymmetric Models

The Minimal Supersymmetric Standard Model (MSSM) is the supersymmetric R-Parity-conserving extension of the Standard Model and it represents the smallest particle content for a supersymmetric theory in which the Standard Model can be embedded.

It basically consists of taking the two-Higgs-doublet extension of the SM and adding the corresponding supersymmetric partners. The MSSM Lagrangian is then constructed by including all possible interaction terms that satisfy the spacetime supersymmetry algebra, $SU(3) \times SU(2) \times U(1)$ gauge invariance and B-L conservation. Finally, the most general soft-supersymmetry-breaking terms are added.

There are a total of 105 new parameters in addition to the SM ones. Moreover supersymmetry should break dynamically, but it is very difficult to construct a realistic model of spontaneously-broken low-energy supersymmetry where the supersymmetry-breaking arises solely as a consequence of the interactions of the particles of the MSSM. A more viable theory consists of at least two distinct sectors:

a "hidden" sector consisting of particles that are completely neutral with respect to the SM gauge group, and a "visible" sector consisting of the particles of the MSSM. SUSY breaking must be communicated to the observed particles by some interaction felt by both. Supersymmetric models differ in how this supersymmetry breaking is transmitted to the visible sector.

In supergravity models (SUGRA) supersymmetry breaking is transmitted to the MSSM via gravity whereas in gauge-mediated supersymmetry breaking, via gauge forces. Many other models exist. Often more restricted forms of theory are evoked for which it's easier to make definite predictions. The most popular of these is minimal supergravity (mSUGRA) for which parameter freedom is drastically reduced by requiring related parameters to be equal at unification scale. Thus, in mSUGRA models there are only five undetermined parameters:

$$m_0 \quad m_{1/2} \quad A_0 \quad \tan(\beta) \quad \text{sgn}(\mu)$$

where, at GUT scale, m_0 represents all scalars masses (squarks, sleptons and Higgs bosons), $m_{1/2}$ is the common mass of all gaugino and Higgsinos, A_0 is the trilinear coupling, $\tan \beta$ is the ratio of the vacuum expectation values of the Higgs doublets and $\text{sgn}(\mu)$ is the sign of the higgsino mass parameter. The Gluino mass is correlated with $m_{1/2}$ and the slepton mass with m_0 .

1.3 SUSY at LHC

If SUSY exists at weak scale, the rich spectrum of SUSY particles is in the mass range to be explored at LHC. The kinds of measurements that can be made depends very much on the SUSY model.

In R-Parity-conserving models the LSP is stable and escapes detection: the events are thus characterised by large missing transverse energy and cannot be fully reconstructed. Thus, to measure squark, slepton and neutralino masses we need to rely on long decay chains and kinematic endpoints.

SUSY cross section at LHC will be dominated by gluinos and squarks, strongly produced in pairs that then decay producing multiple jets and leptons.

The most studied decay chain is the decay of a gluino to the lightest neutralino via three successive two-body decay: $\tilde{g} \rightarrow q\bar{q} \rightarrow q\bar{q}\chi_2^0 \rightarrow q\bar{q}l\bar{l} \rightarrow q\bar{q}l\bar{l}\tilde{\chi}_1^0$

Neutralinos are invisible and hence it's important to determine the shape of the invariant mass distribution of the di-lepton system: the position of the threshold provides a handle on the absolute mass scale of the particles involved.

In all LHC SUSY simulations, the main background to SUSY is SM: in fact the SM background is considered to be relatively small. The main problem is then to separate the many SUSY processes that occur; it is essential, particularly in hadron collisions, to generate all the processes which are kinematically allowed and not just specific channels of interest. Many different points in the parameter space of

different models are chosen to study the various possible signatures which might face the experiment.

2 SUSY studies

2.1 Data sample

As said, the first step in any SUSY simulation is to generate the full spectrum of the model. Since the signal at LHC will hopefully have large cross sections, hard cuts against the SM can be used without reducing drastically the event rate.

The input files used as signal samples for the work presented here were generated with ISAJET7.71 for a particular point (SU3) in the parameter space of the mSUGRA model. Namely, the values of the five parameters are:

$$m_0 = 100 \text{ GeV} \quad m_{1/2} = 300 \text{ GeV} \quad A_0 = -300 \text{ GeV} \quad \tan(\beta) = 6 \quad \text{sgn}(\mu) = +$$

This is a generic point with no specific mass degeneracies in the "Bulk" region (cross section = 19.3 pb). For this point, the masses of the gluino and the two neutralinos are:

$$\tilde{g} = 719.85 \text{ GeV} \quad \tilde{\chi}_2^0 = 223.63 \text{ GeV} \quad \tilde{\chi}_1^0 = 118.94 \text{ GeV}$$

Even though SU3 has already been ruled out by experiments (LEP would have discovered the light Higgs with mass of 111 GeV), it represents a benchmark scenario for SUSY full simulation studies: the simulation of events corresponding to this point has been, in fact, repeated with different software releases.

The data samples I made use of, were generated from full-simulation data and converted into SusyView format.

For this analysis, the SusyView ntuples were processed with SFrame, a HEP cycle-based analyses package based on ROOT.

2.2 l^+l^- signatures

As previously explained, it's possible to pick out particular multi-body decay modes and then to determine combinations of masses by measuring the endpoints of the visible mass distribution. The end point of the dilepton mass spectrum of the decay $\tilde{\chi}_2^0 \rightarrow \tilde{\chi}_1^0 l^+ l^-$ provides a measurement of the $\chi_2^0 - \chi_1^0$ mass difference.

Thus, events were selected to have two opposite-sign leptons correlated in flavour and:

- Missing Et > 100 GeV;
- $|\eta| < 2.5$;

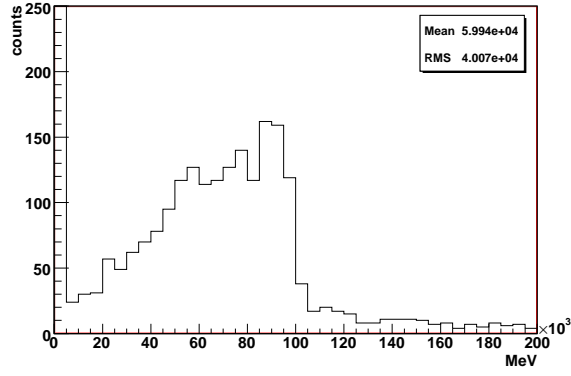


Figure 1: Dilepton mass distribution

- $Pt > 20 \text{ GeV}$.

The resulting dilepton distribution for the signal is shown in fig.1: the endpoint is very clear and the edge is in good agreement with the expected value of $104,69 \text{ GeV}$. The visible peak around the origin needs further investigation.

2.3 Recostruction of gluinos and squarks

The decay examined in the previous section come primarily from $\tilde{g} \rightarrow \tilde{\chi}_2^0 q \bar{q}$, where the gluino may be produced directly or from squark decay. To extract these signals, events were selected with two opposite-sign leptons combined with two hard jets ($Pt > 125 \text{ GeV}$) and the usual additional requirements:

- Missing Et $> 100 \text{ GeV}$;
- $|\eta| < 2.5$;
- $Pt > 20 \text{ GeV}$.

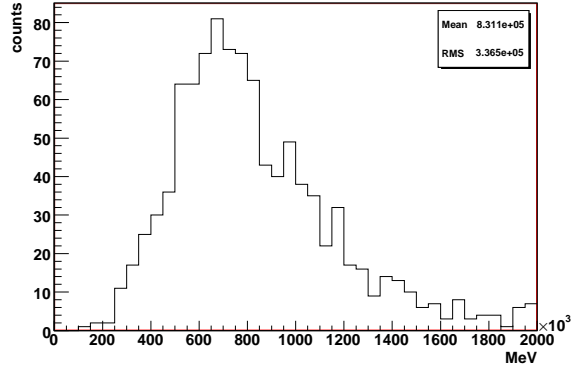


Figure 2: $qq l^+ l^-$ invariant mass distribution

The resulting qql^+l^- mass distribution is shown in fig.2 and its endpoint is supposedly sensitive to the mass difference $M_{\tilde{g}} - M_{\tilde{\chi}_1^0}$. The expected value is $M_{\tilde{g}} - M_{\tilde{\chi}_1^0} = 600 \text{ GeV}$. However, the peak this time is very broad and the shape has no clear structure. This may be caused by large combinatorial background. Since the branching ratio for $\tilde{g} \rightarrow \tilde{\chi}_2^0 b\bar{b} = 6.5\%$, it is also relevant to select b-tagged jets.

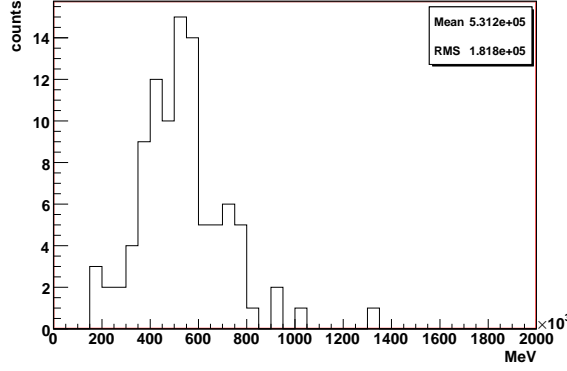


Figure 3: bbl^+l^- invariant mass distribution

In fig.3 is shown the same distribution as in fig.2 but for b-tagged jets: in this case something more similar to a kinematic endpoint is visible around the expected value of 600.91 GeV .

The results shown in this section are consistent with those presented on the ATLAS TDR.

3 Trigger efficiency

The selection of interesting physics signals requires the identification of objects that can be distinguished from the high particle density environment.

The ATLAS trigger system architecture is based on three on-line levels, each of them refining the output of the previous level and adding additional selection criteria. The first level is called Level 1 (L1) and is a hardware trigger with a fixed latency of $2.5\mu s$ which makes its fast selection only using fragments of the events from a subset of detectors and very rough selection criteria.

The second and third levels are software triggers called Level 2 (L2) and Event Filter (EF) with average latency of $10ms$ and $1s$, respectively. L2 is provided by L1 with information of the position and transverse momentum of candidate objects. In comparison with L1, L2 applies more sharp selection criteria. The main task of EF is to refine L2 selection. EF is the only level that works with the complete detector data. L2 and EF are often referred to as high level trigger (HLT).

SUSY spectrum with its small mass gaps and long decay chains is a difficult

physics scenario for the trigger. Hence, simulation of trigger precision and efficiency needs detailed study.

3.1 l^+l^- signatures

To see how developed and precise the algorithms for the trigger are, it's possible to look at the results obtained using only events processed and accepted by the trigger and compare these with those from "hand-made" cuts applied with SFrame, previously shown. The $qq l^+l^-$ and $bb l^+l^-$ invariant mass distributions shown in Fig.4 -5 have been measured using only the events which passed both the L2 and the EF trigger for jet multiplicity = 2 and $P_t > 120 GeV$.

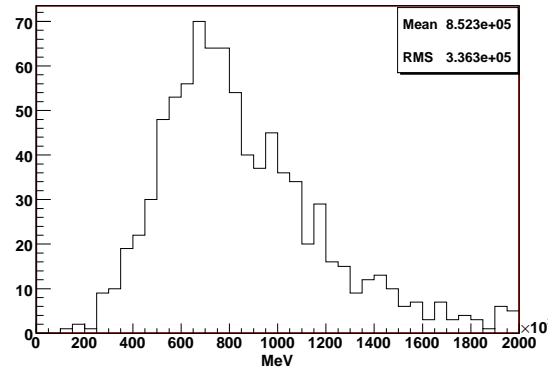


Figure 4: $qq l^+l^-$ invariant mass distribution for events which passed L2 and EF triggers for $n>2$ jets and jet $P_t > 120 GeV$

The means of the distributions appear shifted of $212 GeV$ compared to those in Fig.2-3. Nevertheless the results are in good agreement.

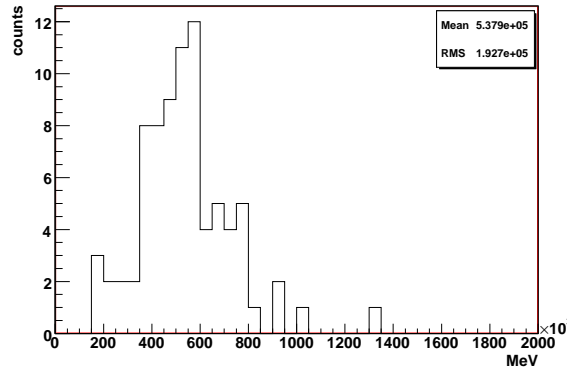


Figure 5: $qq l^+l^-$ invariant mass distribution for events which passed L2 and EF triggers for $n>2$ b-tagged jets and jet $P_t > 120 GeV$

3.2 Trigger efficiency and turn-on curves

Hard QCD jets are very interesting objects for the search of new physics. Nevertheless, there's no unequivocal definition for the objects called "jets". Since the effective masses of the squarks and gluino or, in general, of the parent particles of a decay chain, depend on the energy and momentum of all the particles of the produced jets, jet reconstruction algorithms play a relevant role.

In the present analysis, I made use of the algorithm Cone 0.4 (sums up over calorimeter activities within a cone of radius 0.4 around the cluster).

In Fig.6 is represented the efficiency for L2 and EF as a function of increasing jet multiplicity (*i.e.* at least 2, 3, 4 jets per event) but with decreasing jet transverse momentum (*i.e.* at least 120, 65 50 GeV per jet). The efficiency of the event selection decreases as the number of jets increases. One consequence of this is, for example, that in the attempt of extracting events belonging to the channel previously discussed (*i.e.* $\tilde{q} \rightarrow q\tilde{\chi}_2^0 \rightarrow q\tilde{l}\tilde{l} \rightarrow qll\tilde{\chi}_1^0$), one would need a trigger that selects events with at least 4 hard jets and the efficiency of this selection would be somewhere close to 50%.

Also visible in the Fig.6, the loss of efficiency for EF compared to that of L2.

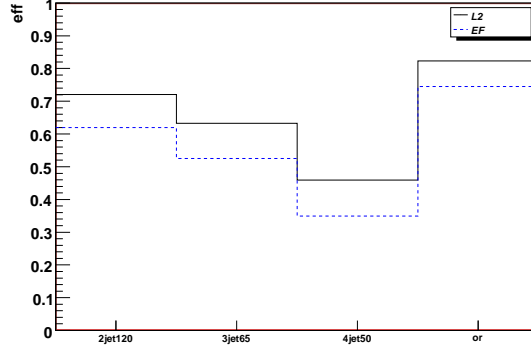


Figure 6: L2 and EF trigger efficiency for events with at least 2, 3 and 4 jet with decreasing Pt. The last bin represents the combined efficiency for either of these triggers

In the attempt of selecting SUSY events, a further understanding of the trigger efficiency is necessary to perform appropriate cuts.

In Fig.7-8-9 are plotted the trigger efficiencies (L1, L2 and EF, respectively) versus the reconstructed momentum of the jets (clockwise: the first, second, third and fourth hardest jet of the event). The same plot for an ideal trigger would be a step function, with the function turning to one at the corresponding value of the trigger

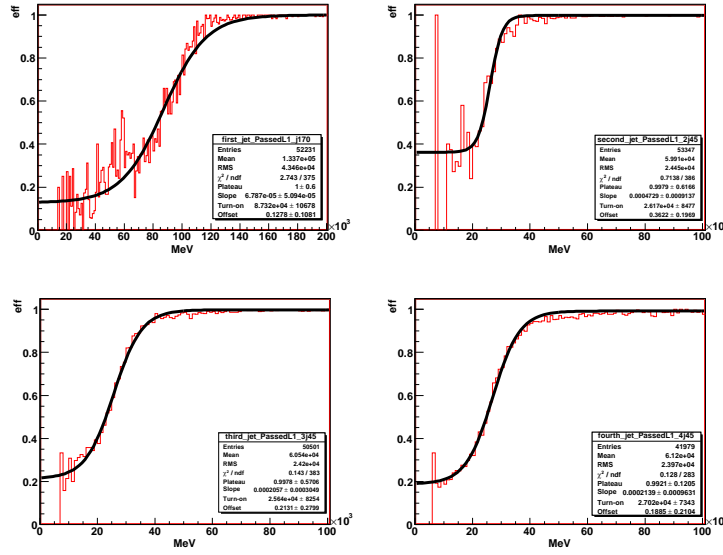


Figure 7: L1 trigger efficiency versus jets transverse momentum for different multiplicity

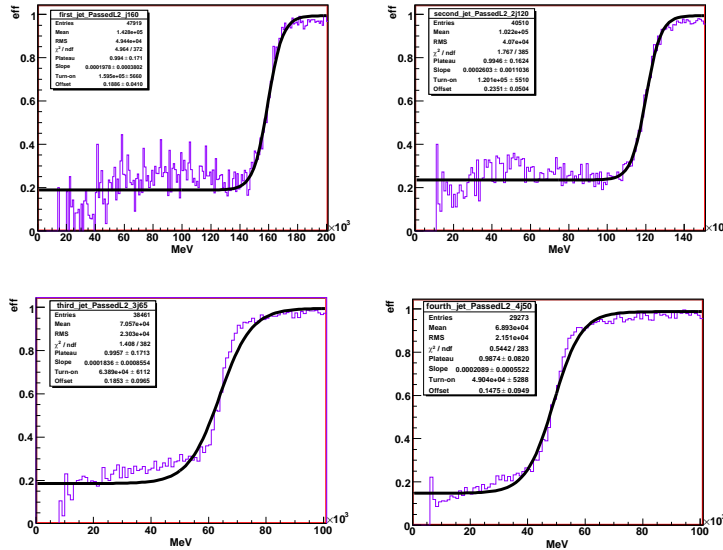


Figure 8: L2 trigger efficiency versus jets transverse momentum for different multiplicity

threshold.

In our case, there is always a non-zero offset, i.e. events that do not fulfill the selection requirements also pass.

The trigger might make its decision to accept or reject an event analysing jet variables reconstructed with a different algorithm.

For example, the momentum of a jet reconstructed using Cone 0.7 algorithm should

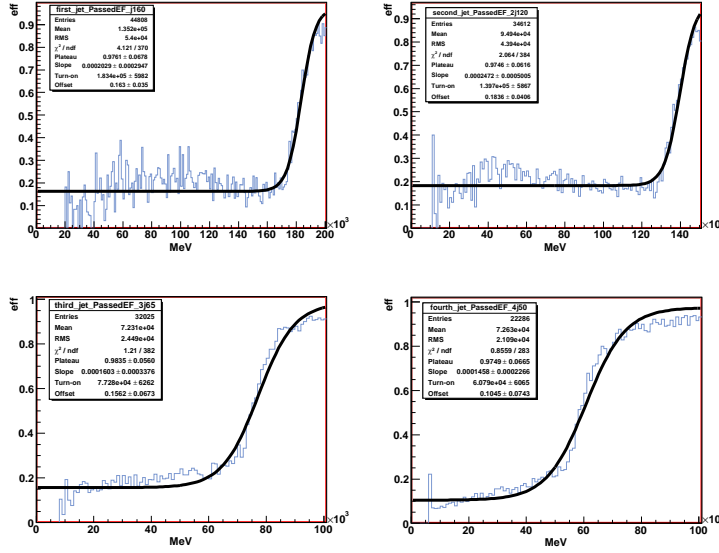


Figure 9: EF trigger efficiency sversus jets transverse momentum for different multiplicity

be higher than that reconstructed with Cone 0.4; since the x-axis of fig.7-8-9 shows the momentum of the jet reconstructed with Cone 0.4 algorithm, event selected with a trigger that uses Cone 0.7 would appear below the selection threshold. This should be double-checked.

The turn-on parameter must converge to the threshold value.

3.3 Missing Transverse Energy Reconstruction

The impossibility of detecting the LSPs (and, in some models, also the NLSP, next lightest SUSY particles) makes the missing energy of an event the basic ingredient of the discovery of a new physics beyond the SM. In hadron machines, the distribution of the energy and longitudinal momentum of the partons cannot be measured. In fact, only the transverse momentum can be used for measurements; it is calculated from the vector sum of energy deposits and it is called missing transverse energy (Et). Fig.10 shows the missing Et provided by the Monte Carlo simulation (Truth) compared with those reconstructed using the total information of the event, L1 and EF algorithms. In particular, the second, third and fourth distributions are the result of the subtraction of the reconstructed energy and the truth value. Obviously, the more these distributions converge the better. Nevertheless, a great shift in the mean is visible, especially in L1 and EF. Anyway, this doesn't represent a real problem since the missing energy scale in the SM processes is much smaller.

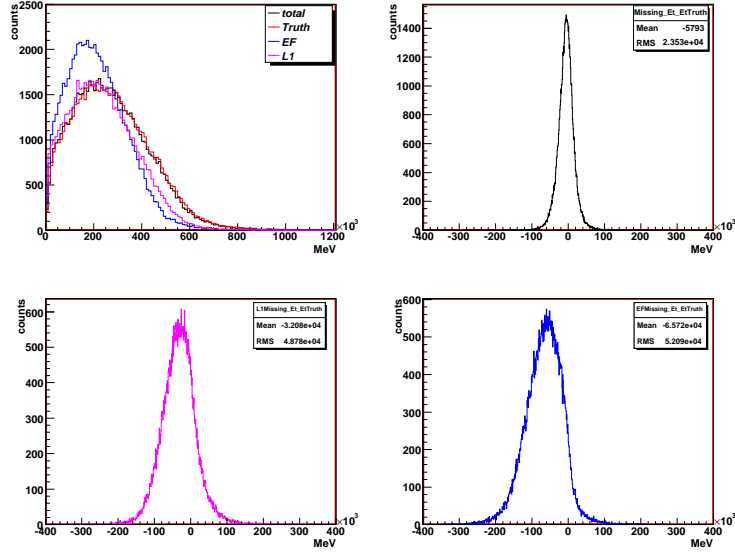


Figure 10: Missing transverse energy from MC truth compared with those reconstructed using the total information of the event, L1 and EF algorithms.

4 Summary

The aim of my work was, firstly, to determine whether the data and tools used in this analyses might be used for further studies on the selection of supersymmetric events in the ATLAS detector.

The reproduced invariant mass distributions shown in the second section of this paper turned out to be in good agreement with previous studies and prove their consistency.

The study then converged on the analyses of the efficiency of the three trigger levels of the ATLAS detector.

The invariant mass distributions for events selected by the HLT shown in the third section, may be a proof of the reliability of the trigger performance whereas the study on the efficiency may be used to find better cuts to be implemented in a future trigger. For further studies a lot more need to be taken into consideration.

References

- [1] H.Murayama, March 2000: Supersymmetry phenomenology,
hep - ph/0002232v2
- [2] H.E.Haber, April 2006: Supersymmetry (Theory,Experiment),
[http//pdg.lbl.gov/2007/reviews/contents_sports.html](http://pdg.lbl.gov/2007/reviews/contents_sports.html)

- [3] ATLAS collaboration, May 1999, ATLAS detector and physics performance TDR
- [4] C.M.Harris, Feb 2005: Physics beyond the Standard Model,
hep - ph/0502005v1
- [5] C.Risler, DESY Zeuthen Summer Students lectures, Aug 13-15, 2007,
[http : //risler.web.cern.ch/risler/](http://risler.web.cern.ch/risler/)